Journal of Molecular Liquids 235 (2017) 17–23

Contents lists available at ScienceDirect

Journal of Molecular Liquids

journal homepage: www.elsevier.com/locate/molliq

The effect of water dynamics on conformation changes of albumin in pre-denaturation state: photon correlation spectroscopy and simulation

N. Atamas [a], V. Bardik [a,*], A. Bannikova [b], O. Grishina [c], E. Lugovskoi [d], S. Lavoryk [e], Y. Makogonenko [d], V. Korolovych [f], D. Nerukh [g], V. Paschenko [h]

[a] Kiev Taras Shevchenko National University, Pr. Gluskova 4, Kiev 03127, Ukraine
[b] Saratov State Vavilov Agrarian University, Bolshaya Sadovaya 220, Saratov 410005, Russia
[c] Molecular Physiology and Biophysics, Baylor College of Medicine, Houston, TX 77030, USA
[d] Palladin Institute of Biochemistry, Leontovicha 9, Kyiv 01601, Ukraine
[e] LLC NanoMedTech, Antonovycha 68, Kyiv 03680, Ukraine
[f] School of Materials Science and Engineering, Georgia Institute of Technology, Atlanta, GA 30332, USA
[g] Systems Analytics Research Institute, Department of Mathematics, Aston University Birmingham, B4 7ET, UK
[h] Kiev Bogomolets National Medical University, Blvd Shevchenko, 13, Kiev 01004, Ukraine

ARTICLE INFO

Article history:
Received 13 October 2016
Received in revised form 25 December 2016
Accepted 6 January 2017
Available online 7 January 2017

ABSTRACT

Water is essential for protein three-dimensional structure, conformational dynamics, and activity. Human serum albumin (HSA) is one of major blood plasma proteins, and its functioning is fundamentally determined by the dynamics of surrounding water. The goal of this study is to link the conformational dynamics of albumin to the thermal motions in water taking place in the physiological temperature range. We report the results of photon correlation spectroscopy and molecular dynamics simulations of HSA in aqueous solution. The experimental data processing produced the temperature dependence of the HSA hydrodynamic radius and its zeta potential. Molecular dynamics reproduced the results of experiments and revealed changes in the secondary structure caused by the destruction of hydrogen bonds in the macromolecule's globule.

1. Introduction and background

The stability of proteins macromolecules, that is the capacity to preserve their biological functions at certain conditions (pH, temperature, the structure of external environment) is an important physicochemical feature. The stability of a protein is defined by its structure as well as the interactions with surrounding molecules. The solvation properties of peptide and protein aqueous solutions have been investigated by various techniques and the fact of the ultimate connection between the dynamical properties of the environment and the protein conformational motions was supported in many experimental and simulation works [1–8]. Recent experimental studies [9–31] focused on the interactions of hydration water with solute protein molecules. These techniques allowed to investigate the static and dynamic properties of the hydration water and their relation with the properties of the hydrated molecules.

Quasi-elastic (QENS) and inelastic neutron scattering (INS), gave a possibility to study rotational and translational motions at the picosecond timescale, and the vibrational density of states of water surrounding proteins and peptides [10–12]. The fast collective dynamics of the biomolecule–solvent mutual interactions have been investigated by Brillouin neutron scattering [13]. The combination of Molecular Dynamics (MD) simulation and QENS has been performed in [14]. It was shown that water dynamics appear spatially heterogeneous in the first hydration shell. Below the critical hydration level the water translational and rotational dynamics are slow in comparison with the bulk water. Molecules of the first hydration layer form structures like a barrier for outer water molecules. The results obtained by INS [15–17] in pico- and nanosecond timescale indicate that the dynamics of the whole biomolecule are affected by the hydration water and surface protein motions are strengthened by the solvent matching those of the breaking and re-formation of hydrogen bonds.

THz spectroscopy has been used to investigate the influence of the water structure on peptides [98] and proteins [19–23]. Based on this technique, the radii of the hydration shells have been detected for such proteins as lysozyme, myoglobin, BSA [20,23] and ubiquitin [21]. The estimations of the hydration shell thickness obtained in [23] are substantiated by NMR studies [24,25], X-ray scattering [26], and neutron scattering [27]. It was shown also [19,22] that water molecules are arranged to form a gradient around 'active' sites and to provide reactions via the active site's 'hydration funnel'. The change in water dynamics [24,25] at the hydration shell can be extended up to 5–8 water layers, which is longer compared to previous findings.

* Corresponding author.
E-mail address: vital@univ.kiev.ua (V. Bardik).

http://dx.doi.org/10.1016/j.molliq.2017.01.017
0167-7322/

The stabilising effects of buried water on the protein structure have been discussed in [28–31]. Single water molecules stabilise protein by filling internal cavities. Backbone residues of loops and other polar atoms interact with the water molecules buried in the protein core. Buried water may also act as lubricant to favour loop dynamics.

Investigations carried out by FTIR spectroscopy have shown that water molecules connecting proton donor to acceptor sites or electron donor to electron acceptor sites facilitate both proton-transfer processes [32] and electron-transfer reactions [33–35]. In both cases, the transfer is faster where the linking water molecules possess stronger hydrogen bonding. Besides, a cluster structure of H-bonds in water plays a catalytic role in water oxidation in photosynthetic oxygen evolution [36].

The intra and inter-helical hydrogen bonds are important determinants of the local protein structure, dynamics, and water interactions. Molecular dynamics simulation and bioinformatics revealed that perturbation of the inter-helical hydrogen bonds can be coupled to rapid changes in water dynamics [37]. In some cases the water wire may be affected by the binding of various ions [38].

Thus the cited studies demonstrate reversible coupling of water dynamics with protein conformational stability. However it remains unsolved what initially plays the major role in conformation dynamics of proteins: surrounding molecules in the 'hydration shell' or physical properties of macromolecule. In other words "…who is the master and who is the slave in the water–macromolecule interaction…" [9].

We directed our attention to one of the aspects connected with the dynamics of surrounding water under temperature effect. As it was shown in a number of papers [39–43] the global hydrogen bonding network in water disintegrates into an ensemble of weakly interacting clusters: dimers, trimers, tetramers, etc. in the vicinity of a specific temperature point $T_H = 42$ °C. In other words, the spatial connectivity between linear molecular chains is disrupted. The value of T_H coincides with the physiological temperature at which the thermal denaturation of many proteins takes place. As denaturation (unfolding) is a form of conformational dynamics of proteins, the dynamics of water in this region can have an effect on the protein's conformational changes. Particularly, it was shown [44] that the conformational changes of human serum albumin (HSA) in the temperature interval 25–55 °C is a process subdivided into three sub-transitions which might be related to the links between the three structured domains of HSA. The sub-transitions are sequential and separated by a temperature interval of approximately 9 °C. The temperature of the last sub-transition coincides with T_H, which is the maximal value of fever in human body at pathological conditions. In our study we tried to correlate the conformational dynamics of HSA (as one of major blood plasma proteins) with the dynamic properties of water in the temperature range 25–45 °C, especially in the vicinity of $T_H \approx 42$ °C as the threshold temperature of protein conformational stability. The size and hydration were related to the structural changes of the protein molecule at different temperatures.

The structure of HSA has been determined by X-ray crystallography at high resolution [45]. Several factors like pH, temperature, etc. can affect its structure and dynamics [46]. HSA plays a special role in transporting metabolites and drug molecules throughout the vascular system and also in maintaining the osmotic pressure of plasma acids, metabolites, and binding of different ligands [47–50]. HSA is a single chain protein with 585 amino-acid residues with a predominant α-helixal heart-shaped structure [48,51].

2. Methodology, results, and discussion

2.1. Photon correlation spectroscopy

We have applied photon correlation spectroscopy (PCS) [52] to obtain the temperature dependences of the hydrodynamic radius and zeta potential. This technique has much research interest due to its wide use in studies of proteins and DNA aqueous solutions [53], aqueous solutions of poly(ethylene glycol) [54], trehalose aqueous solutions [55–57], alcohols and semidiluted polymer solutions [58–60], cluster growth in aqueous sugars and glass-forming aqueous glucose solutions [61,62]. The comparative studies of PCS and incoherent quasi-elastic neutron scattering (IQENS) on hydrogenous systems such as polymeric aqueous solutions, alcohols and homologous disaccharide aqueous solutions have been presented in [63,64]. PCS technique showed that water behaved as a good solvent and furnished the temperature evolution of the hydration number. IQENS revealed the presence of entangled water and evidenced the effects of H-bond on the diffusive motions. The comparison of the rotational relaxation times, obtained by IQENS and PCS separated the self-particle contribution from the collective one.

In the process of measurement we obtain the second order correlation function or so called normalised autocorrelation function 'intensity-intensity', defined as

$$G^2(\tau) = \langle I(0)I(\tau)\rangle / \langle I\rangle^2, \tag{1}$$

where, I is the total scattered intensity. In the case of non-interacting particles the relationship between the second order and the first order correlation functions takes place

$$G^2(\tau) = 1 + \alpha\left|G^1(\tau)\right|^2, \tag{2}$$

For diffusing monodisperse spherical particles, the normalised field autocorrelation function takes a simple exponential form

$$G^{(1)}(\tau) = \exp\{-2q^2D\tau\}, \tag{3}$$

where, D is the diffusion coefficient, τ is time, $q = 4\pi n/\lambda \sin(\frac{\theta}{2})$, λ is the vacuum wavelength of the laser, n is the refractive index of the solution, θ is the scattering angle.

2.1.1. Hydrodynamic radius

As it was noticed in [63,64] at low concentrations of proteins the diffusion coefficient can be connected to the macromolecular hydrodynamic radius by the Einstein-Stokes relation

$$R_H = kT/6\pi\eta D, \tag{4}$$

where, η is the dispersant viscosity, T is temperature, k is the Boltzmann constant. However, polymeric solutions with macromolecules at high molecular weight can be considered as polydisperse, in this case a standard cumulant analysis is more suitable for processing the data [52,60]. This technique used in the spectrometer Zetasizer Nano ZS (ZEN3600) [52]. Aqueous solutions of HSA at concentrations 1 mg/ml with NaCl ions (0,075 mol/l, 0,15 mol/l, 0,225 mol/l) were investigated. The measurements were performed in the temperature interval 25–50 °C with the 1 °C step. The set of measurements were carried out using commercial spectrometer Zetasizer Nano ZS (ZEN3600).

The cumulant analysis gives a good description of the radius that is comparable with other methods for spherical, reasonably narrow monomodal samples (monomodal sample contains only particles of one size), that is with polydispersity below the value of 0.1. For samples with a slightly increased distribution width, the Z-average size and polydispersity gives values that can be used for comparative purposes. For broader distributions, where the polydispersity is over 0.5, it is unwise to rely on the Z-average mean, and a distribution analysis should be used to determine the peak positions. In our study the index of polydispersity was 0.1 ± 0.05. The values of the hydrodynamic radii obtained from the Z-average diffusion coefficient (formula (4)) in the temperature interval 30–50 °C are presented in Fig. 1. The value of the hydrodynamic radius is unchanged in the investigated temperature range. The concentration of NaCl ions does not affect R_H, and the value equals approximately 5 ± 0.3 nm, that does not exceed the experimental precision of Zetasizer (0.5 nm).

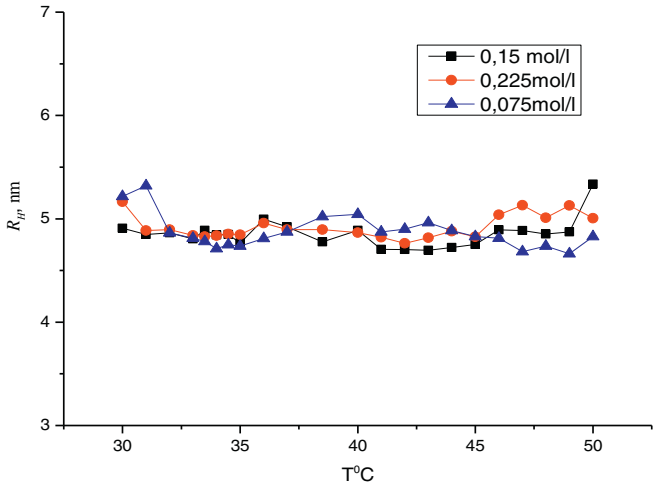

Fig. 1. Temperature dependence of the macromolecular hydrodynamic radius R_H at different concentrations of NaCl.

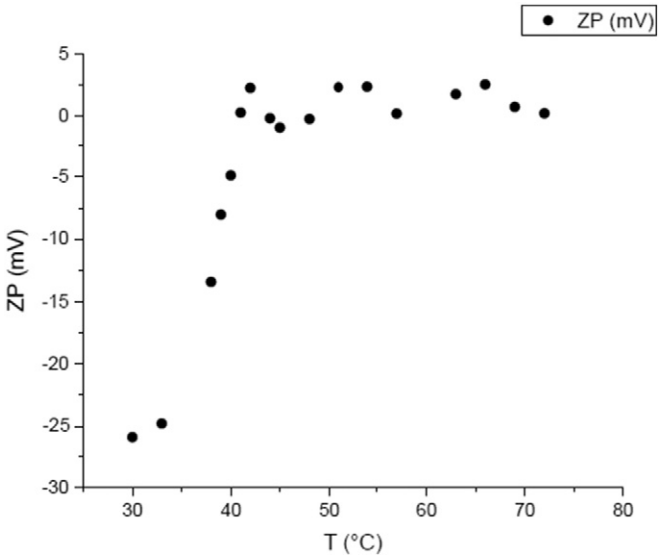

Fig. 2. Temperature dependences of the zeta potential (ZP) for albumin aqueous solution.

2.1.2. Zeta potential (ZP)

In order to correlate water dynamic in the 'hydration shell' with conformational changes of a macromolecule we investigated the temperature influence on ZP of an aqueous solution. The ZP can be considered as a key parameter that describes the surface charge on protein and characterises its hydration layer [65–69]. The charge distribution at the macromolecule surface affects the dynamics of ions in the surrounding interfacial region. By convention the liquid layer surrounding the macromolecule may be subdivided into two parts: an inner region (the Stern layer), where surrounding molecules and the ions are strongly bound with the protein macromolecule and an outer, diffuse, region where they are less firmly attached. An electrical double layer surrounds each macromolecule. In the Stern layer the protein macromolecule move together with the surrounding molecules and the ions, beyond the inner layer, in the diffusive region, the surrounding molecules do not drift together with the macromolecule. There is a boundary between the Stern and diffusive layers. This boundary is the surface of hydrodynamic shear or so called slipping plane. The potential which exists at this boundary is the ZP.

The ZP was obtained using electrophoretic light scattering technique based on the measurement of electrophoretic mobility. The ZP of the particle can be calculated by the application of the Henry equation

$$\mu_r = \frac{2\varepsilon_r \varepsilon_0 \varsigma f(Ka)}{3\eta},$$

where, μ_r is the electrophoretic mobility, ε_r is the relative permittivity/dielectric constant, ε_0 is the permittivity of vacuum, ζ is the zeta potential, $f(Ka)$ is the Henry's function and η is viscosity at experimental temperature. Electrophoretic determinations of the zeta potential are most commonly done in aqueous media and moderate electrolyte concentration and two values of $f(Ka)$ are generally accepted as approximations, either 1.5 or 1.0 $f(Ka)$. The accuracy in defining the electrophoretic mobility is $0.12 \cdot 10^{-8}$ $m^2/V \cdot s$ (for particles diameter in measurements range: 3.8 nm–100 μm), hence the error for the zeta potential does not exceed approximately 5%.

Temperature and pH are most important factors affecting ZP. In our study we have been carried out the measurements at fixed pH 7 and concentration of NaCl (0,075 mol/l). This value of pH corresponds to the value of the zeta potential approximately −27 mV at the temperature 30 °C. The values of the ZP in the temperature range 25–70 °C are presented in the Fig. 2.

Based on the presented data we can conclude that the change of the ZP with temperature is a two-stage process. On the first stage we observe the decrease of the ZP magnitude: starting from −27 mV and temperature 35 °C up to zero value of the ZP in the vicinity of the temperature point 42 °C. Thus, zero value of the ZP or the isoelectric point (IEP) is located in the close proximity of 42 °C. It should be noted that the system is not particularly stable in a region surrounding the condition of IEP. Then the value of the ZP varies from −2.5 mV to 2.5 mV up to the denaturation temperature.

2.2. Simulation

The dynamics of HSA macromolecule in aqueous solution at different temperatures was simulated using the multifunction package HARLEM, which combines the methods of molecular and Brownian dynamics. The crystallographic structure (PDB entry 1AO6) [45] of albumin at the resolution of 2.5 Å was used. The albumin macromolecule consists of 585 amino-acid residues, 17 pairs of disulfide bridges, and one free cysteine (Fig. 3).

The initial structure for the simulation was prepared by solvating the protein macromolecule (5672 atoms) with 118,722 water molecules of the fixed density in a cubic cell with the edge of 20 nm. To avoid additional stresses, structure energy minimisation in vacuum was implemented over 10,000 steps for each model. Minimisation of protein

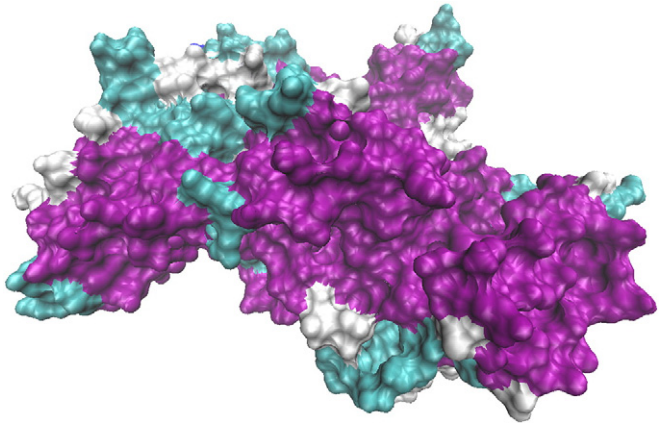

Fig. 3. Visualization of the albumin crystallographic structure from PDB [45]. Components of the regular secondary structure are shown: α-helix – purple, turn – cyan, coil – white.

with water was carried out over 20,000 steps using the descent method and the conjugate gradients scheme. The Langevin thermostat was used to fix momenta with a collision frequency of 2:0. The initial temperature was set 4 K and then increased by 20 K at every simulation step up to 304 K. The preparatory simulation duration was 50 ps.

At the next stage, the obtained optimised model was investigated by molecular dynamics (MD). MD simulations were performed for 50 ns for every model with given temperature. The data were saved every 10 ps. Periodic boundary conditions were applied with a constant pressure of 1 atm, using the Amber 99 force field, the cutoff for non-bonded interactions was set to 12 Å. The TIP3P water model with unfixed inner degree of freedom was used. Electrostatic interactions were calculated using the particle mesh Ewald molecular dynamics (PMEMD) [70–72]. Intramolecular bonds were constrained using the SHAKE algorithm [73]. The Berendesen thermostat with the time constant (relaxation time) of 2 ps was applied in order to maintain temperature.

2.2.1. Gyration radius

The values of the gyration radius was calculated in the above mentioned temperature range (Fig. 4). The radius of gyration was defined by the formula given below on the basis of the crystallographic data [45] for atom coordinates and their changes under temperature effect

$$R_g^2 = \sum m_i r_i^2 / \sum m_i, \quad (5)$$

where, m_i is the mass of the i-th atom in the macromolecule and r_i is the distance from the centre of mass to the i-th atom.

Both hydrodynamic and gyration radii remain unchanged within random fluctuations in the temperature range 25–50 °C. As one can see they approximately differ from each other by 1.5 nm, which coincide with the values of the hydration shell reported in [20,23]. This difference has natural explanation. By definition the hydrodynamic radius measured by PCS is the radius of a hypothetical hard sphere that diffuses with the same speed as the macromolecule. In reality, such hard sphere does not exist. Macromolecules in solution are non-spherical, dynamic, and solvated. The hydrodynamic radius calculated from the diffusional properties of the macromolecule is indicative of the *apparent* size of the dynamic hydrated/solvated particle. Whereas, as it was mentioned above, the gyration radius is the average distance from the center of mass to the macromolecular surface [74].

At the next stage we have analysed the temperature effect in the vicinity of 42 °C on the distances between the sulfur atoms (Sγ) in pairs of cysteines and COO-groups of asparaginic or glutamic acids and NH_3-groups of lysine or arginine (salt bridges).

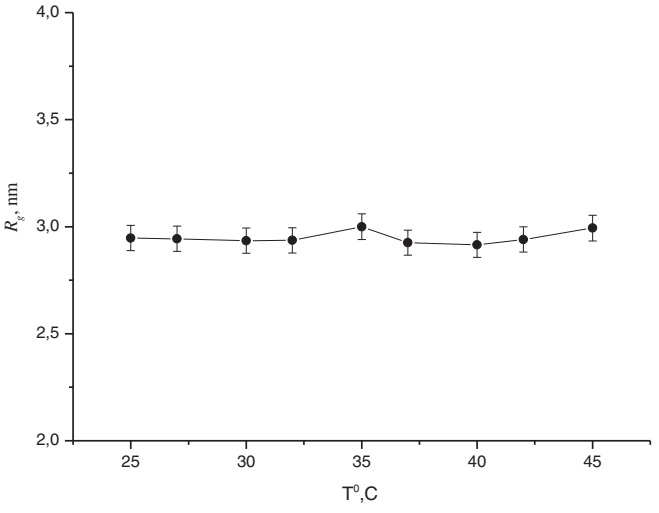

Fig. 4. Temperature dependence of the gyration radius calculated from the simulation data.

Disulfide bonds (bridges) or SS bonds are covalent bonds formed from two thiol groups [75,76]. The effect of SS bonds on the protein structural stability, dynamics, correlated motion, and flexibility of local residues has been investigated experimentally [77–80] and computationally [81–87]. Three necessary conditions were formulated [88] for cysteine pairs to be involved in SS bonds: a bond length of 2.05 ± 0.3 Å, an angle between the sulfur atoms and β-carbon atom of 103°, and an orientation of the two β-carbon atoms corresponding to a rotation of ±90° about the SS bonds. In [87] atomistic MD simulation of HSA with and without SS bonds have been carried out. The authors have shown that the removal of SS bonds mainly destabilises the tertiary structure, and the removal of some of them affected the secondary structure of the macromolecule.

Initially, the equilibrium distances between S_γ atoms in the presence of SS bonds were defined as 2.05 ± 0.03 Å (1AO6 [45]). Destabilising changes occurred after 35 ns of simulation. The distances between S_γ atoms reached above 5 Å and mostly below 10 Å, but in some pairs of cysteine distances increased up to 15 Å. The results of simulation for distances between S_γ atoms are presented in Supplementary information and some of them in Fig. 5. As one can see SS bonds are not changed by temperature as the lengths of disulfide bridges are stable and correspond to one of the Creighton requirements [88], namely the distances between S_γ atoms to be 2.05 ± 0.03 Å.

Salt bridges represent a combination of two noncovalent bonds: the hydrogen bond and the electrostatic interactions. Noncovalent bonds are considered to be relatively weak interactions, but these interactions add up to make an important contribution to the overall stability of proteins [89]. The salt bridge derives from the anionic carboxylate of either aspartic acid or glutamic acid and the cationic ammonium from lysine or the guanidinium of arginine [90]. The distances between the residues participating in the salt bridge are considered important. The length of salt bridge is approximately 4 Å. Lengths greater than this distance do not qualify as forming a salt bridge [91]. We have analysed the temperature effect on the salt bridge length for 40 pairs of residues. Most pairs of residues have distances of about 4 Å with a standard deviation of 0.5 (Supplementary information).

Minor fluctuations of the distance with temperature have been observed for the pair of GLU530-LYS499, the value was changing from 3.5 Å at temperature 25 °C up to 2.5 Å at temperature 45 °C, but in general, most of distances between amino-acid residues forming the salt bridge have the constant value in the temperature range 25–45 °C. The error at calculation of both distances between S_γ atom and the lengths of the salt bridges was 0.07 Å.

The dynamics of amino-acid residues with decreasing temperature were studied by calculating of root-mean-square deviation

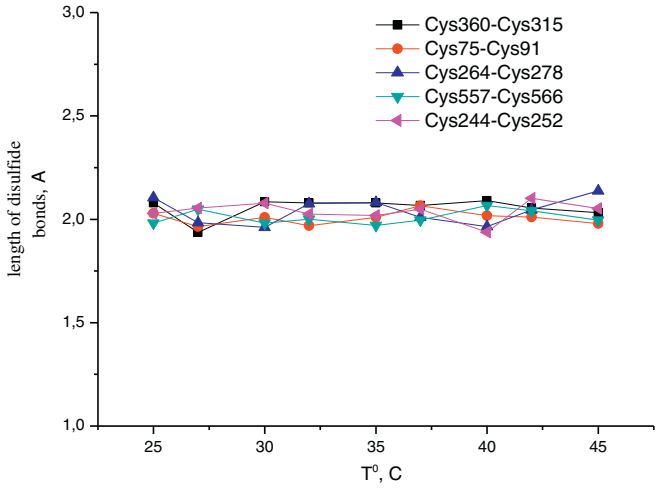

Fig. 5. The temperature dependence of distances between S_γ atoms in cysteines pairs.

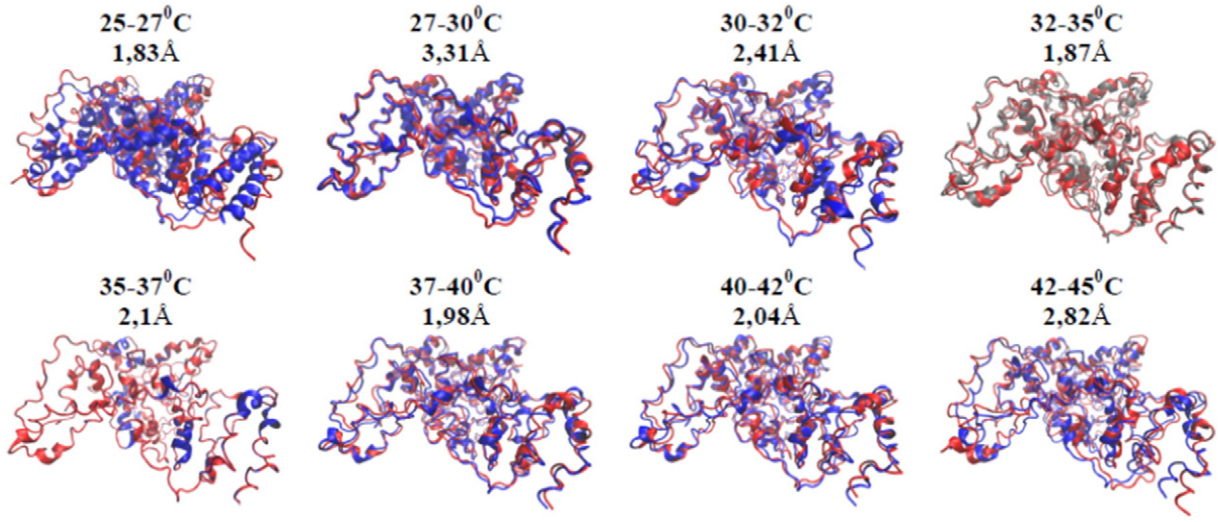

Fig. 6. Cartoon representation of the amino-acids residue displacements and the RMSD values corresponding to every temperature interval. Blue and silver colours correspond to the conformational state in the first temperature point, red indicates the conformational state in the second temperature point for every snap-shot. The visualization was created using Visual Molecular Dynamics (VMD).

(RMSD). Evaluation of the RMSD allows us to investigate the conformational changes of the structure by comparing the residue positions in the reference points. The RMSD values were calculated for close conformational states in specified temperature points with respect to the initial structure (PDB). The residues displacements and the values of RMSD are presented in Fig. 6.

Thus, the structure of the macromolecule does not undergo significant transformations with the temperature increase, we observe only slight deflection of the RMSD values with respect to the reference temperature in the certain temperature interval. The average value of the RMSD for all temperature range is 2.3 Å. The simulation of the HSA structure [87] without SS bonds gave the RMSD value 4.5 Å. Some previous MD studies [92–97] reported values ranging from 2 to 10 Å, at those for stable structures from 2 to 3 Å [96].

The simulation of the temperature effect on the conformation stability has shown structural changes in secondary structures of HSA (Fig. 7). Conformational changes take place in the components of the regular secondary structures, which are stabilized by hydrogen bonds. Most the structural rearrangements are observed in the α-helix. The α-helix is maintained by the hydrogen bonds between the hydrogen and oxygen atoms of peptides groups. Thus conformational changes in the α-helix are governed by the hydrogen bonds destruction in the investigated temperature range 25–45 °C.

3. Conclusions

The results presented here demonstrate that the conformation changes of albumin are ultimately correlated with water dynamics in the vicinity of the temperature point 42 °C. On the one hand the experimental (hydrodynamic radius) and simulation (gyration radius, stability of disulfide bonds and salt bridges) data support the fact of the macromolecule is stabile in the temperature range 25-50 °C with approximately the same size. The value of the gyration radius obtained from molecular dynamics is supported by the results in [20,23]. The difference in 1.5 nm between the hydrodynamic and gyration radii is proved. Additionally, this value coincides with the estimation of the hydration layer thickness obtained by THz spectroscopy [20]. Thus, this suggests that the hydrodynamic radius includes both solvent and shape effects. We obtain, on the basis of comparison of the simulation and PCS data, a well-established value of the hydration layer thickness.

On the other hand the zeta potential behaviour from temperature 35 °C up to denaturation indicates that the hydration layer beyond the

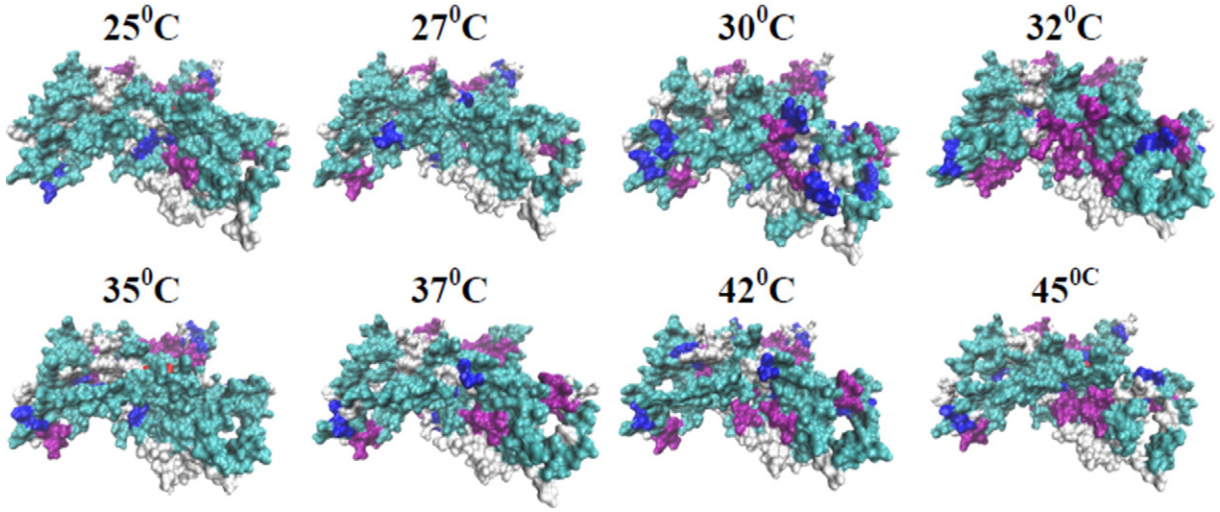

Fig. 7. Visualization of conformation changes with temperature. Components of the regular secondary structure: α-helix – purple, 3_{10}-helix – blue, turn – cyan, coil – white, π-helix - red.

Stern layer (an inner region, where surrounding molecules and the ions are strongly bound with the protein macromolecule of HSA) is drastically changed in the vicinity of 42 °C. The temperature dependence of the zeta potential for HSA may imply conformational changes in the macromolecule structure, surface modifications, and, as a result the initial stage of denaturation process. In this context the simulation data just revealed the conformational changes of the secondary structures, which are stabilized namely by hydrogen bonds. Thus it can mean that the temperature range 40–42 °C is the initial stage of denaturation for HSA.

For deeper understanding of the water collective dynamics around the protein and the correlation with conformation changes we are planning to apply and develop the methods based on Linear Stochastic Estimation [98]. We reserved also, for the future work, the Molecular Dynamics simulation of the temperature effect on the retardation factor [9], which is the relation of the characteristic times in the bulk water and the hydration layer. This important parameter is used to quantify the correlations between the conformational changes of the macromolecule and the dynamics of the water shell.

Appendix A. Supplementary data

Supplementary data to this article can be found online at http://dx.doi.org/10.1016/j.molliq.2017.01.017.

References

[1] R. Abseher, H. Schreiber, O. Steinhauser, The influence of a protein on water dynamics in its vicinity investigated by molecular dynamics simulation, Proteins: Struct., Funct., Bioinf. 25 (1996) 366–378.
[2] V.A. Makarov, B.K. Andrews, P.E. Smith, B.M. Pettitt, Residence times of water molecules in the hydration sites of myoglobin, Biophys. J. 79 (2000) 2966–2974.
[3] A. Garcia, G. Hummer, Water penetration and escape in proteins, Proteins Struct. Funct. Genet. 38 (2000) 261–272.
[4] M. Tarek, D. Tobias, Role of protein-water hydrogen bond dynamics in the protein dynamical transition, Phys. Rev. Lett. 88 (2002) 138101.
[5] F. Pizzitutti, M. Marchi, F. Sterpone, P.J. Rossky, How protein surfaces induce anomalous dynamics of hydration water, J. Phys. Chem. B 111 (2007) 7584–7590.
[6] H. Frauenfelder, G. Chen, J. Berendzen, P.W. Fenimore, H. Jansson, B.H. McMahon, I.R. Stroec, J. Swenson, R.D. Young, A unified model of protein dynamics, PNAS 106 (2009) 5129–5134.
[7] F. Sterpone, G. Stirnemann, D. Laage, Magnitude and molecular origin of water slowdown next to a protein, J. Am. Chem. Soc. 134 (2012) 4116–4119.
[8] O. Rahaman, S. Melchionna, D. Laage, F. Sterpone, The effect of protein composition on hydration dynamics, Phys. Chem. Chem. Phys. 15 (2013) 3570–3576.
[9] L. Comez, M. Paolantoni, P. Sassi, S. Corezzi, A. Morresi, D. Fioretto, Molecular properties of aqueous solutions: a focus on the collective dynamics of hydration water, The Royal Society of Chemistry. Soft Matter 12 (2016) 5501–5514, http://dx.doi.org/10.1039/c5sm03119b.
[10] A. Frolich, F. Gabel, M. Jasnin, U. Lehnert, D. Oesterhelt, A.M. Stadler, M. Tehei, M. Weik, K. Wood, G. Zaccai, From shell to cell: neutron scattering studies of biological water dynamics and coupling to activity, Faraday Discuss. 141 (2009) 117–130.
[11] D. Russo, R.K. Murarka, J.R.D. Copley, T. Head-Gordon, Molecular view of water dynamics near model peptides, J. Phys. Chem. B 109 (2005) 12966–12975.
[12] S. Khodadadi, J.H. Roh, A. Kisliuk, E. Mamontov, M. Tyagi, S.A. Woodson, R.M. Briber, A.P. Sokolov, Dynamics of biological macromolecules: not a simple slaving by hydration water, Biophys. J. 98 (2010) 1321–1326.
[13] A. Orecchini, A. Paciaroni, A.D. Francesco, C. Petrillo, F. Sacchetti, Collective dynamics of protein hydration water by brillouin neutron spectroscopy, J. Am. Chem. Soc. 131 (2009) 4664–4669.
[14] D. Russo, G. Hura, T. Head-Gordon, Hydration dynamics near a model protein surface, Biophys. J. 86 (2004) 1852–1862.
[15] A. Orecchini, A. Paciaroni, A.R. Bizzarri, S. Cannistraro, Dynamics of different hydrogen classes in β-lactoglobulin: a quasielastic neutron scattering investigation, J. Phys. Chem. B 106 (2002) 7348–7354.
[16] A. Paciaroni, A. Orecchini, E. Cornicchi, M. Marconi, C. Petrillo, M. Haertlein, M. Moulin, H. Schober, M. Tarek, F. Sacchetti, Fingerprints of amorphous icelike behavior in the vibrational density of states of protein hydration water, Phys. Rev. Lett. 101 (2008) 148104.
[17] A. Paciaroni, E. Cornicchi, M. Marconi, A. Orecchini, C. Petrillo, M. Haertlein, M. Moulin, F. Sacchetti, Coupled relaxations at the protein–water interface in the picosecond time scale, J. R. Soc. Interface 6 (2009) S635–S640.
[18] B. Born, H. Weingartner, E. Brundermann, M. Havenith, Solvation dynamics of model peptides probed by terahertz spectroscopy. Observation of the onset of collective network motions, J. Am. Chem. Soc. 131 (2009) 3752–3755.
[19] V.C. Nibali, M. Havenith, New insights into the role of water in biological function: studying solvated biomolecules using terahertz absorption spectroscopy in conjunction with molecular dynamics simulations, J. Am. Chem. Soc. 136 (2014) 12800–12807.
[20] J.W. Bye, S. Meliga, D. Ferachou, G. Cinque, J.A. Zeitler, R.J. Falconer, Analysis of the hydration water around bovine serum albumin using terahertz coherent synchrotron radiation, J. Phys. Chem. A 118 (2014) 83–88.
[21] B. Born, S.J. Kim, S. Ebbinghaus, M. Gruebele, M. Havenith, The terahertz dance of water with the proteins: the effect of protein flexibility on the dynamical hydration shell of ubiquitin, The Royal Society of Chemistry. Faraday Discuss. 141 (2009) 161–173.
[22] Y. Xu, M. Havenith, Perspective: watching low-frequency vibrations of water in biomolecular recognition by THz spectroscopy, J. Chem. Phys. 143 (2015) (170901-1-7).
[23] O. Sushko, R. Dubrovka, R.S. Donnan, Sub-terahertz spectroscopy reveals that proteins influence the properties of water at greater distances than previously detected, J. Chem. Phys. 142 (2015) (055101-1-9).
[24] C. Mattea, J. Qvist, B. Halle, Dynamics at the protein-water Interface from ^{17}O spin relaxation in deeply supercooled solutions, Biophys. J. 95 (2008) 2951–2963.
[25] J. Qvist, E. Persson, C. Mattea, B. Halle, Time scales of water dynamics at biological interfaces: peptides, proteins and cells, Faraday Discuss. 141 (2009) 131–144.
[26] D.I. Svergun, S. Richard, M.H.J. Koch, Z. Sayers, S. Kuprin, G. Zaccai, Protein hydration in solution: experimental observation by X-ray and neutron scattering, Proc. Natl. Acad. Sci. U. S. A. 95 (1998) 2267–2272.
[27] A. Pertsemlidis, A.M. Saxena, A.K. Soper, T. Head-Gordon, R.M. Glaeser, Direct evidence for modified solvent structure within the hydration shell of a hydrophobic amino acid, Proc. Natl. Acad. Sci. U. S. A. 93 (1996) 10769–10774.
[28] K. Takano, Y. Yamagata, K. Yutani, Buried water molecules contribute to the conformational stability of a protein, Protein Eng. 16 (2003) 5–9.
[29] S. Park, J.G. Saven, Statistical and molecular dynamics studies of buried waters in globular proteins, Proteins: Struct., Funct., Bioinf. 60 (2005) 450–463.
[30] O. Carugo, Statistical survey of the buried waters in the protein data bank, Amino Acids 48 (2016) 93–202, http://dx.doi.org/10.1007/s00726-015-2064-4.
[31] O. Carugo, Structure and function of water molecules buried in the protein core, Curr. Protein Pept. Sci. 16 (2015) 259–265.
[32] F. Garczarek, K. Gerwert, Functional waters in intraprotein proton transfer monitored by FTIR difference spectroscopy, Nature 439 (2005) 109–112.
[33] J. Lin, I.A. Balabin, D.N. Beratan, The nature of aqueous tunneling pathways between electron-transfer proteins, Science 310 (2005) 1311–1313.
[34] A. de la Lande, N.S. Babcock, J. Řezáč, B.C. Sanders, D.R. Salahub, Surface residues dynamically organize water bridges to enhance electron transfer between proteins, PNAS 107 (2010) 11799–11804.
[35] C.F.A. Negre, G.E. Jara, D.M.A. Vera, A.B. Pierini, C.G. Sánchez, Detailed analysis of water structure in a solvent mediated electron tunneling mechanism, J. Phys. Condens. Matter 23 (2011) 245305.
[36] B.C. Polander, B.A. Barry, A hydrogen-bonding network plays a catalytic role in photosynthetic oxygen evolution, PNAS 109 (2012) 6112–6117.
[37] C. del Val, L. Bondar, A.-N. Bondar, Coupling between inter-helical hydrogen bonding and water dynamics in a proton transporter, J. Struct. Biol. 186 (2014) 95–111.
[38] T. Jiang, W. Han, M. Maduke, E. Tajkhorshid, Molecular basis for differential anion binding and proton coupling in the Cl^-/H^+ exchanger ClC-ec1, J. Am. Chem. Soc. 138 (2016) 3066–3075.
[39] A.I. Fisenko, N.P. Malomuzh, To what extent is water responsible for the maintenance of the life for warm-blooded organisms? Int. J. Mol. Sci. 10 (2009) 2383–2411.
[40] T.V. Lokotosh, S. Magazu, G. Maisano, N.P. Malomuzh, Nature of self-diffusion and viscosity in supercooled liquid water, Phys. Rev. E 62 (2000) 3572–3580.
[41] A.I. Fisenko, N.P. Malomuzh, A.V. Oleynik, To what extent are thermodynamic properties of water argon-like? Chem. Phys. Lett. 450 (2008) 297–301.
[42] L.A. Bulavin, A.I. Fisenko, N.P. Malomuzh, Surprising properties of the kinematic shear viscosity of water, Chem. Phys. Lett. 453 (2008) 183–187.
[43] T.V. Lokotosh, N.P. Malomuzh, K.N. Pankratov, Thermal motion in water + electrolyte solutions according to quasi-elastic incoherent neutron scattering data, J. Chem. Eng. Data 55 (2010) 2021–2029.
[44] M. Rezaei-Tavirani, S.H. Moghaddamnia, B. Ranjbar, M. Amani, S.A. Marashi, Conformational study of human serum albumin in pre-denaturation temperatures by differential scanning calorimetry, circular dichroism and UV spectroscopy, J. Biochem. Mol. Biol. 39 (2006) 530–536.
[45] S. Sugio, A. Kashima, S. Mochizuki, M. Noda, K. Kobayashi, Crystal structure of human serum albumin at 2.5 Å resolution, Protein Eng. 12 (1999) 439–446.
[46] J.R. Brown, in: V.M. Rosenoer, M. Oratz, M.A. Rothschild (Eds.), Albumin Structure, Function and Uses, Pergamon Press, Oxford, UK, 1977.
[47] M.A. Rothschild, M. Oratz, S.S. Schreiber, Serum albumin, Hepatology 8 (1988) 385–401.
[48] D.C. Carter, J.X. Ho, Structure of serum albumin, Adv. Protein Chem. 45 (1994) 153–203.
[49] F. Kratz, Albumin as a drug carrier: design of prodrugs, drug conjugates and nanoparticles, J. Control. Release 132 (2008) 171–183.
[50] M. Rozga, W. Bal, The Cu(II)/Aβ/human serum albumin model of control mechanism for copper-related amyloid neurotoxicity, Chem. Res. Toxicol. 23 (2010) 298–308.
[51] D.C. Carter, X.-M. He, S.H. Munson, P.D. Twigg, K.M. Gernert, M.B. Broom, T.Y. Miller, Three-dimensional structure of human serum albumin, Science 244 (1989) 1195–1198.
[52] H.Z. Cummins, E.R. Pike, Photon Correlation and Light Beating Spectroscopy, Plenum Press, New York and London, 1974 (Published in cooperation with NATO Scientific Affairs Division).
[53] S. Magazu, G. Maisano, F. Mallamace, N. Micali, Growth of fractal aggregates in water solutions of macromolecules by light scattering, Phys. Rev. A 39 (1989) 4195–4200.
[54] D.I. Donato, M.P. Janelli, S. Magazu, G. Maisano, D. Majolino, P. Migliardo, R. Ponterio, Viscosity and photon correlation spectroscopy measurements in aqueous solutions of poly(ethylene glycol), J. Mol. Struct. 381 (1996) 213–217.
[55] S. Magazù, G. Maisano, P. Migliardo, V. Villari, Experimental simulation of macromolecules in trehalose aqueous solutions: a photon correlation spectroscopy study, J. Chem. Phys. 111 (1999) 9086–9092.
[56] C. Branca, S. Magazù, G. Maisano, P. Migliardo, V. Villari, A.P. Sokolov, The fragile character and structure-breaker role of alpha, alpha trehalose: viscosity and Raman scattering findings, J. Phys. Condens. Matter 11 (1999) 3823–3832.

[57] S. Magazù, G. Maisano, P. Migliardo, E. Tettamanti, V. Villari, Transport phenomena and anomalous glass-forming behaviour in alpha, alpha-trehalose aqueous solutions, Mol. Phys. 96 (1999) 381–387.
[58] M.P. Jannelli, S. Magazu, P. Migliardo, U. Wanderlingh, Chain length dependence and H-bond effects on diffusive processes of alcohols by IQENS, DLS and NMR, Phys. B Condens. Matter 234 (1997) 355–356.
[59] M.P. Jannelli, S. Magazu, P. Migliardo, F. Aliotta, E. Tettamanti, Transport properties of liquid alcohols investigated by IQENS, NMR and DLS studies, J. Phys. Condens. Matter 8 (1996) 8157–8171.
[60] A. Faraone, S. Magazu, G. Maisano, R. Ponterio, V. Villari, Experimental evidence of slow dynamics in semidilute polymer solutions, Macromolecules 32 (1999) 1128–1133.
[61] D.L. Sidebottom, Ultraslow relaxation of hydrogen-bonded dynamic clusters in glass-forming aqueous glucose solutions: a light scattering study, Phys. Rev. E 76 (2007) 011505.
[62] D.L. Sidebottom, T.D. Tran, Universal patterns of equilibrium cluster growth in aqueous sugars observed by dynamic light scattering, Phys. Rev. E 82 (2010) 051904.
[63] S. Magazù, IQENS - dynamic light scattering complementarity on hydrogenous systems, Physica B 226 (1996) 92–106.
[64] S. Magazù, F. Migliardo, M.T.F. Telling, Study of the dynamical properties of water in disaccharide solutions, Eur. Biophys. J. Biophys. Lett. 36 (2007) 163–171.
[65] A. Sze, D. Erickson, L. Ren, D. Li, Zeta-potential measurement using the Smoluchowski equation and the slope of the current–time relationship in electroosmotic flow, J. Colloid Interface Sci. 261 (2003) 402–410.
[66] K. Fischer, M. Schmidt, Pitfalls and novel applications of particle sizing by dynamic light scattering, Biomaterials 98 (2016) 79–91.
[67] S. Bhattacharjee, DLS and zeta potential – what they are and what they are not? J. Control. Release 235 (2016) 337–351.
[68] M. Předota, M.L. Machesky, D.J. Wesolowski, Molecular origins of the zeta potential, Langmuir 32 (2016) 10189–10198.
[69] S.R. Maduar, A.V. Belyaev, V. Lobaskin, O.I. Vinogradova, Electrohydrodynamics near hydrophobic surfaces, Phys. Rev. Lett. 114 (2015) 118301.
[70] T. Darden, D. York, L. Pedersen, Particle mesh Ewald: an N log(N) method for Ewald sums in large systems, J. Chem. Phys. 98 (1993) 10089–10092.
[71] U. Essmann, L. Perera, M.L. Berkowitz, T. Darden, H. Lee, L.G. Pedersen, A smooth particle mesh Ewald method, J. Chem. Phys. 103 (1995) 8577–8593.
[72] M. Crowley, T. Darden, T. Cheatham, D. Deerfield, Adventures in improving the scaling and accuracy of a parallel molecular dynamics program, J. Supercomput. 11 (1997) 255–278.
[73] J.-P. Ryckaert, G. Ciccotti, H.J.C. Berendsen, Numerical integration of the Cartesian equations of motion of a system with constraints: molecular dynamics of n-alkanes, J. Comput. Phys. 23 (1977) 327–341.
[74] C.M. Kok, A. Rudin, Relationship between the hydrodynamic radius and the radius of gyration of a polymer in solution, Die Makromolekulare Chemie, Rapid Communications, 2, Wiley Online Library 1981, pp. 655–659.
[75] W. Wang, C.J. Roberts, Aggregation of Protein Therapeutics, John Wiley & Sons, Hoboken, NJ, 2010.
[76] N.J. Bulleid, L. Ellgaard, Multiple ways to make disulfides, Trends Biochem. Sci. 36 (2011) 485–492.
[77] A. Cooper, S.J. Eyles, S.E. Radford, C.M. Dobson, Thermodynamic consequences of the removal of a disulphide bridge from hen lysozyme, J. Mol. Biol. 225 (1992) 939–943.
[78] E. Drakopoulou, J. Vizzavona, J. Neyton, V. Aniort, F. Bouet, H. Virelizier, A. Menez, C. Vita, Consequence of the removal of evolutionary conserved disulfide bridges on the structure and function of charybdotoxin and evidence that particular cysteine spacings govern specific disulfide bond formation, Biochemistry 37 (1998) 1292–1301.
[79] K.S. Siddiqui, A. Poljak, M. Guilhaus, G.D. Feller, S. Amico, C. Gerday, R. Cavicchioli, Role of disulfide bridges in the activity and stability of a cold-active α-amylase, J. Bacteriol. 187 (2005) 6206–6212.
[80] D.C. Vaz, J.R. Rodrigues, W. Sebald, C.M. Dobson, R.M.M. Brito, Enthalpic and entropic contributions mediate the role of disulfide bonds on the conformational stability of interleukin-4, Protein Sci. 15 (2006) 33–44.
[81] M.E. Moghaddam, H. Naderi-Manesh, Role of disulfide bonds in modulating internal motions of proteins to tune their function: molecular dynamics simulation of scorpion toxin Iqh-III, Proteins: Struct., Funct., Bioinf. 63 (2006) 188–196.
[82] M. Qin, J. Zhang, W. Wang, Effects of disulfide bonds on folding behavior and mechanism of the β-sheet protein tendamistat, Biophys. J. 90 (2006) 272–286.
[83] Y.L. Tsai, H.-W. Chen, T. Lin, W.-Z. Wang, Y.-C. Sun, Molecular dynamics simulation of folding of a short helical toxin peptide, J. Theor. Comput. Chem. 06 (2007) 213–221.
[84] M. Aschi, A. Bozzi, R. Di Bartolomeo, R. Petruzzelli, The role of disulfide bonds and n-terminus in the structural properties of hepcidins: insights from molecular dynamics simulations, Biopolymers 93 (2010) 917–926.
[85] J.R. Allison, G.-P. Moll, W.F. van Gunsteren, Investigation of stability and disulfide bond shuffling of lipid transfer proteins by molecular dynamics simulation, Biochemistry 49 (2010) 6916–6927.
[86] A. Godwin, J.-W. Choi, E. Pedone, S. Balan, R. Jumnah, S. Shaunak, S. Brocchini, M. Zloh, Molecular dynamics simulations of proteins with chemically modified disulfide bonds, Theor. Chem. Accounts 117 (2007) 259–265.
[87] M.M. Castellanos, C.M. Colina, Molecular dynamics simulations of human serum albumin and role of disulfide bonds, J. Phys. Chem. B 117 (2013) 11895–11905.
[88] T.E. Creighton, Disulphide bonds and protein stability, BioEssays 8 (1988) 57–63.
[89] D.E. Anderson, W.J. Becktel, F.W. Dahlquist, pH-induced denaturation of proteins: a single salt bridge contributes 3–5 kcal/mol to the free energy of folding of t4 lysozyme, Biochemistry 29 (1990) 2403–2408.
[90] D.A. Dougherty, Modern Physical Organic Chemistry, University Science Books, Sausalito, CA, 2006.
[91] S. Kumar, R. Nussinov, Close-range electrostatic interactions in proteins, ChemBioChem 3 (2002) 604–617.
[92] J. Li, X. Zhu, C. Yang, R. Shi, Characterization of the binding of angiotensin ii receptor blockers to human serum albumin using docking and molecular dynamics simulation, J. Mol. Model. 16 (2010) 789–798.
[93] S.I. Fujiwara, T. Amisaki, Molecular dynamics study of conformational changes in human serum albumin by binding of fatty acids, Proteins: Struct., Funct., Bioinf. 64 (2006) 730–739.
[94] B. Sudhamalla, M. Gokara, N. Ahalawat, D.G. Amooru, R. Subramanyam, Molecular dynamics simulation and binding studies of β-sitosterol with human serum albumin and its biological relevance, J. Phys. Chem. B 114 (2010) 9054–9062.
[95] M. Rueda, C. Ferrer-Costa, T. Meyer, A. Perez, J. Camps, A. Hospital, J.L. Gelpi, A.M. Orozco, A consensus view of protein dynamics, Proc. Natl. Acad. Sci. U. S. A. 104 (2007) 796–801.
[96] O. Deeb, M.C. Rosales-Hernández, C. Gómez-Castro, R. Garduño-Juárez, J. Correa-Basurto, Exploration of human serum albumin binding sites by docking and molecular dynamics flexible ligand–protein interactions, Biopolymers 93 (2010) 161–170.
[97] R. Artali, G. Bombieri, L. Calabi, A. Del Pra, A molecular dynamics study of human serum albumin binding sites, II Farmaco 60 (2005) 485–495.
[98] D. Nerukh, S. Karabasov, Water-peptide dynamics during conformational transitions, J. Phys. Chem. Lett. 4 (2013) 815–819.